THE BELL SYSTEM TECHNICAL JOURNAL
Vol. 52, No. 9, November, 1973
Printed in U.S.A.

Multimode Theory of Graded-Core Fibers

By D. GLOGE and E. A. J. MARCATILI

(Manuscript received March 29, 1973)

New technologies of fiber manufacture and a demand for unusual fiber qualities in communication systems have intensified the interest in a comprehensive theory of multimode fibers with nonuniform index distributions. This paper deals with a general class of circular symmetric profiles which comprise the parabolic distribution and the abrupt core-cladding index step as special cases. We obtain general results of useful simplicity for the impulse response, the mode volume, and the near- and far-field power distributions. We suggest a modified parabolic distribution for best equalization of mode delay differences. The effective width of the resulting impulse is more than four times smaller than that produced by the parabolic profile. Of course, practical manufacturing tolerances are likely to influence this distribution. A relation is derived between the maximum index error and the impulse response.

I. INTRODUCTION

Conventional optical fibers consist of a high-index core surrounded by a cladding of lower index. The index step between core and cladding contains the light inside the core and isolates it from the outer fiber surface, whose quality is usually difficult to control. In a more general way, inside guidance can be accomplished by any index profile which decreases from a maximum inside the fiber to a lower (cladding) value. The specific shape of the profile has an effect on the distribution of the guided optical power in the fiber and on the overall loss encountered, but, more importantly, the profile profoundly influences the velocities of the various propagating modes. A good example is the parabolic index distribution which was predicted to nearly equalize the group velocities of the propagating modes.[1,2] The Selfoc fiber which closely approximates these conditions has indeed since exhibited an extremely narrow impulse response.[3,4]

These effects greatly enhance the chances of multimode fibers to be used in optical communication systems. On the other hand, a theory

of the interrelations between index profile, impulse response, and power distribution is presently only available for the two special cases of the uniform and the parabolic core index. This paper provides a more general theory and studies a broad class of index profiles potentially useful in communication applications. The uniform and the parabolic profile are special cases within this class.

Our concern with multimode fibers for communication applications allows us to make four simplifying assumptions:

(*i*) The index profile is circular symmetric.
(*ii*) The core diameter measures hundred wavelengths or more and, hence, a great number of modes can propagate.
(*iii*) The total index change within the guiding core region is only a few hundredths, so the propagating modes can be considered essentially as transverse electromagnetic.[5]
(*iv*) Index variations within the distance of a wavelength are negligible, and the conditions of geometrical optics (or the zeroth order of the WKB method) apply.

Except for these four restrictions and the requirement of guidance, the index profile can be of the most general form. It can, for example, have an index depression in the center and one or several ring-shaped index maxima.[6]

For the sake of clarity, this paper is restricted to the simpler type of profile illustrated in Fig. 1. We assume the index profile will decrease monotonically from the center and converge into a flat cladding region which guarantees isolation from the outside surface.

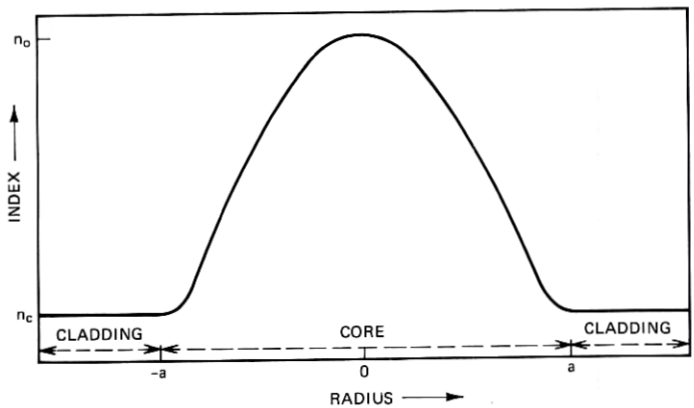

Fig. 1—Cross-sectional sketch of circular symmetric index profile in multimode fiber.

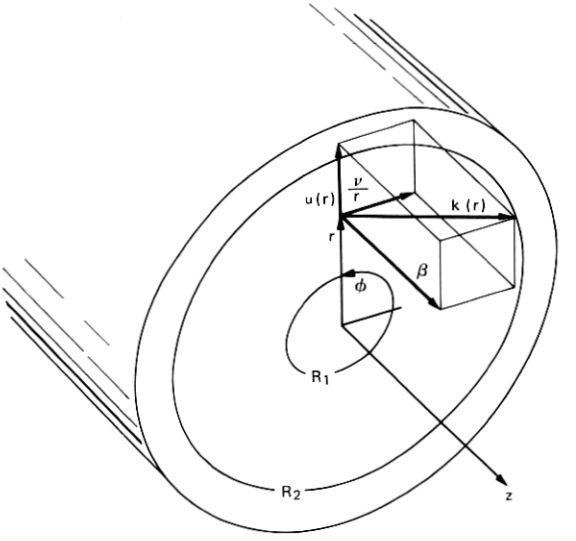

Fig. 2—Wave vector diagram in the propagating region of a multimode fiber.

Apart from the index profile, there are, of course, other influences which affect the impulse response and the optical power distribution inside the fiber. Mode excitation, loss differences in the process of propagation, and coupling among the modes play a part. To isolate the effect of the index profile, we assume here the ideal case of uniform loss, absence of coupling, and equal and simultaneous excitation of all propagating modes at the input. For the computation of the impulse response, the input is assumed to be an infinitely narrow pulse of unit energy.

II. MODE DESIGNATION AND MODE COUNT

All guided modes are essentially transverse electromagnetic and, with some proviso, can be decomposed into linearly polarized pairs.[5,7] Because of the circular symmetry of the index n, the modes have a circular periodicity and can be identified in the conventional way by an azimuthal order number ν. To characterize the radial field distribution, we need an additional mode number μ. The propagation constant β of a particular mode (μ, ν) can then be approximately determined by the WKB method.[6,8] Figures 2 and 3 give a physical description of these relationships. In Fig. 2, the local wave number

$$k(r) = 2\pi n(r)/\lambda \tag{1}$$

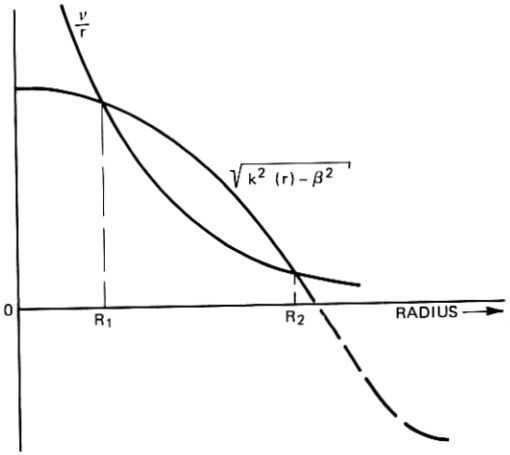

Fig. 3—Sketch defining regions of periodic and aperiodic field characteristics of a mode of azimuthal order ν.

is decomposed into its components in a cylindrical coordinate system (r, ϕ, z). The unknown radial component becomes

$$u(r) = [k^2(r) - \beta^2 - \nu^2/r^2]^{\frac{1}{2}}. \tag{2}$$

Given β and ν, we can find two radii R_1 and R_2, at which $u(r)$ vanishes (see Fig. 3). These radii define a ring-shaped region within which u is real, causing a radial periodicity of the mode field. Outside this region, the field is aperiodic.

Radially decreasing (or evanescent) field conditions obtain outside, when the phase inside (approximately) adds up to an integer number of half periods between R_1 and R_2. Consequently, if μ designates this number of half periods,

$$\mu\pi = \int_{R_1}^{R_2} u(r)dr = \int_{R_1}^{R_2} [k^2(r) - \beta^2 - \nu^2/r^2]^{\frac{1}{2}}dr. \tag{3}$$

We would have obtained the same result by way of the WKB method, with the only difference that μ and ν^2 would be replaced by $\mu + \frac{1}{4}$ and $\nu^2 + \frac{1}{4}$. These corrections are important in the case of small μ or ν, and particularly for the fundamental mode which has $\mu = \nu = 0$. On the other hand, to obtain a general view of the mode structure, we can ignore the $\frac{1}{4}$-terms as long as we refrain from discussing individual low-order modes.

For the purpose of a total mode count, let us consider the limits of μ, ν, and β. The requirement of evanescent field conditions in the

cladding (index n_c in Fig. 1) limit β to a minimum value

$$\beta_c = 2\pi n_c/\lambda. \tag{4}$$

Modes with smaller β find propagating conditions in the cladding and are no longer bounded by the core profile. Condition (4) defines mode cutoff. The largest value for ν results for $\beta = \beta_c$ and $\mu = 0$, and alternatively μ is largest for $\beta = \beta_c$ and $\nu = 0$. We obtain the total number of modes M from a summation of (3) over all ν from 0 to ν_{max}. If ν_{max} is a large number, we may consider ν a continuous variable and replace the sum by an integral. In this case,

$$M = \frac{4}{\pi}\int_0^{\nu_{max}} \int_{R_1(\nu)}^{R_2(\nu)} [k^2(r) - \beta_c^2 - \nu^2/r^2]^{\frac{1}{2}} dr d\nu . \tag{5}$$

The factor 4 in front of the expression allows for the fact that each combination μ, ν designates a (degenerate) group of four modes of different polarization or orientation.[5] Figure 4 illustrates the area of the double integration indicated in (5). A change of order in the integration leads to

$$M = \frac{4}{\pi}\int_0^a \int_0^{r(k^2-\beta_c^2)^{\frac{1}{2}}} (k^2 - \beta_c^2 - \nu^2/r^2)^{\frac{1}{2}} d\nu dr , \tag{6}$$

where a is the radius at which the index $n(r)$ reaches the cladding value n_c. Integrating (6) with respect to ν yields

$$M = \int_0^a [k^2(r) - \beta_c^2]^{\frac{1}{2}} r dr = \left(\frac{2\pi}{\lambda}\right)^2 \int_0^a [n^2(r) - n_c^2]^{\frac{1}{2}} r dr . \tag{7}$$

For small index differences, the integral represents the volume under the (circular symmetric) profile plot. It may be worth noting, though, that the substance of this relation is not limited to circular symmetry.

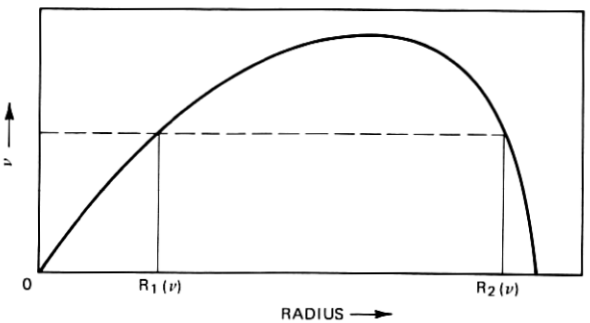

Fig. 4—Region of double integration in eq. 5.

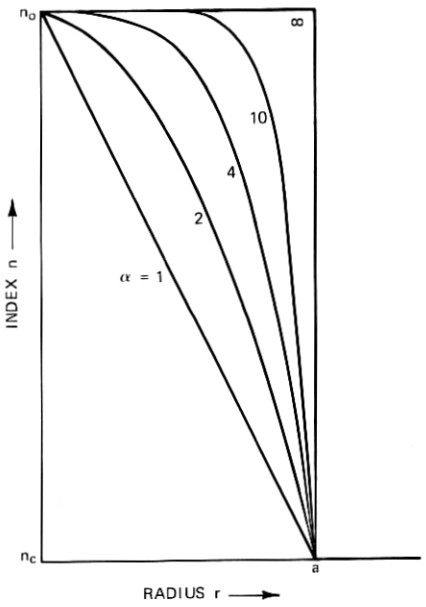

Fig. 5—A few of the index profiles defined by $n = n_0[1 - 2\Delta(r/a)^\alpha]^{\frac{1}{2}}$ for small Δ.

For later use we write (7) in the somewhat different form

$$m(\beta) = \int_0^{R_2(0)} [k^2(r) - \beta^2]^{\frac{1}{2}} r dr , \tag{8}$$

where $m(\beta)$ denotes the number of modes having a propagation constant larger than β. The upper limit $R_2(0)$ of the integration is the radius at which $k(r) = \beta$.

Let us now consider a particular class of profiles defined by

$$n(r) = \begin{cases} n_o[1 - 2\Delta(r/a)^\alpha]^{\frac{1}{2}} & \text{for} \quad r < a \\ n_o[1 - 2\Delta]^{\frac{1}{2}} & \text{for} \quad r > a , \end{cases} \tag{9}$$

where α is a parameter between 1 and ∞. Figure 5 illustrates the cases $\alpha = 1, 2, 4, 10$, and ∞. All profiles reach a constant cladding value at $r = a$. The core profile has a cone shape for $\alpha = 1$, becomes nearly parabolic for $\alpha = 2$, and converges to the case of the step profile for $\alpha = \infty$. Using (1) we introduce (9) into (8) and obtain

$$m(\beta) = a^2 \Delta k_o^2 \frac{\alpha}{\alpha + 2} \left(\frac{k_o^2 - \beta^2}{2\Delta k_o^2} \right)^{(2/\alpha)+1} , \tag{10}$$

where

$$k_o = 2\pi n_o/\lambda. \tag{11}$$

For $\beta = \beta_c$ from (4), the total mode number becomes

$$M = \frac{\alpha}{\alpha + 2} a^2 k_o^2 \Delta . \tag{12}$$

It is proportional to the index difference and the core cross section. The uniform profile accepts twice as many modes as the parabolic one and three times more than the cone-shaped one.

III. IMPULSE RESPONSE

Consider all modes to be excited by the same narrow pulse at the input. Each mode transports an equal amount of energy to the fiber end. The individual pulses are expected to suffer a certain distortion, depending on the β–ω characteristic of each mode and dispersion in the dielectric. We assume, however, that the resultant broadening is small, or at least not much larger than the group delay differences between adjacent modes. Because of this effect and other limitations in the system response, the pulses from individual modes are likely to fuse into one continuous output pulse called the impulse response. Since all modes carry the same energy, the power profile of the impulse response is equal to the mode density per unit time interval. In the following theory, the continuity of the impulse response results not from the broadening of the individual mode responses, but from the assumption that μ and ν are continuous functions.

The straightforward method of computing the impulse response starts from (3) to find the propagation constant β for each pair, μ, ν. The group delay in a fiber of length L is then

$$\tau(\mu, \nu) = \frac{Ln_o}{c} \frac{d\beta(\mu, \nu)}{dk_o} , \tag{13}$$

where c is the vacuum velocity of light. A simplification of this approach for the purpose of numerical computations is indicated in the appendix. Once $\tau(\mu, \nu)$ is known, the impulse response results from a count of the combinations μ, ν which arrive between τ and $\tau + d\tau$. This number plotted versus τ then constitutes the impulse response.

For the special class of profiles defined by (9), group delay and impulse response can be computed in a much simpler way. First we postulate that, in this case, the relation between τ and β according to (13) is independent of μ and ν. If this holds—and we shall prove it

later with the help of eq. (16)—we can replace β by τ in (3) and still perform the same integration over ν which led to (8) and, more specifically, to (10). Solving the result of this integration for τ yields

$$\tau = \frac{Ln_o}{c} \frac{d}{dk_o} \left[k_o^2 - \left(\frac{2m}{a^2} \frac{\alpha + 2}{\alpha} \right)^{\alpha/(\alpha+2)} (2\Delta k_o^2)^{2/(\alpha+2)} \right]^{\frac{1}{2}}. \tag{14}$$

This result can easily be verified by solving (10) for β and introducing it into (13). With the help of (10) and the abbreviation

$$\delta = \tfrac{1}{2}(1 - \beta^2/k_o^2), \tag{15}$$

eq. (14) takes the form

$$\tau = \frac{Ln_o}{c} \frac{1 - 4\delta/(\alpha + 2)}{(1 - 2\delta)^{\frac{1}{2}}}. \tag{16}$$

This expression proves indeed to depend on β alone (and not explicitly on m), thus justifying the approach chosen.

To obtain the impulse response, we can now introduce (16) into (10) and differentiate with respect to τ. Although this is not difficult to do, it leads to rather unwieldy expressions. We shall therefore merely consider some special cases of interest. To normalize the impulse response for total unit energy, we divide (10) by (12) and obtain

$$\frac{m}{M} = \left(\frac{\delta}{\Delta} \right)^{(2/\alpha)+1}. \tag{17}$$

Furthermore, since δ can at most assume the value Δ (for $\beta = \beta_c$) and is therefore small compared to unity within the scope of our theory, we develop (16) into a power series in terms of δ and obtain

$$\tau = \frac{Ln_o}{c} \left(1 + \frac{\alpha - 2}{\alpha + 2} \delta + \frac{3\alpha - 2}{\alpha + 2} \frac{\delta^2}{2} \right). \tag{18}$$

We relate τ to the total propagation time Ln_o/c and introduce a new time reference, which ignores the delay common to all modes. Hence,

$$t = \frac{\tau c}{Ln_o} - 1 = \frac{\alpha - 2}{\alpha + 2} \delta + \frac{3\alpha - 2}{\alpha + 2} \frac{\delta^2}{2}. \tag{19}$$

In this time frame, the fundamental mode arrives at $t = 0$.

As long as α is not too close to 2, the linear term in (19) dominates. Therefore,

$$\delta = \begin{cases} \dfrac{\alpha + 2}{\alpha - 2} t & \text{except for } \alpha \approx 2 \\ \sqrt{2t} & \text{for } \alpha = 2. \end{cases} \tag{20}$$

Insert this into (17) and differentiate with respect to t to obtain the impulse response

$$\frac{1}{M}\frac{dm}{dt} = \begin{cases} \dfrac{\alpha+2}{\alpha}\left|\dfrac{\alpha+2}{\alpha-2}\dfrac{1}{\Delta}\right|^{(2/\alpha)+1}|t|^{2/\alpha} & \text{except for } \alpha \approx 2 \\ \dfrac{2}{\Delta^2} & \text{for } \alpha = 2. \end{cases} \tag{21}$$

As δ varies from 0 to Δ, the time t changes from 0 to

$$T = \begin{cases} \dfrac{\alpha-2}{\alpha+2}\Delta & \text{except for } \alpha \approx 2 \\ \dfrac{\Delta^2}{2} & \text{for } \alpha = 2. \end{cases} \tag{22}$$

Outside of this time interval, the impulse response is zero. Figure 6 shows plots of (21) for the profiles sketched in Fig. 5. A change from $\alpha = \infty$ to $\alpha = 10$, which implies a relatively small change in the profile, narrows the impulse response by $\frac{1}{3}$. The response becomes

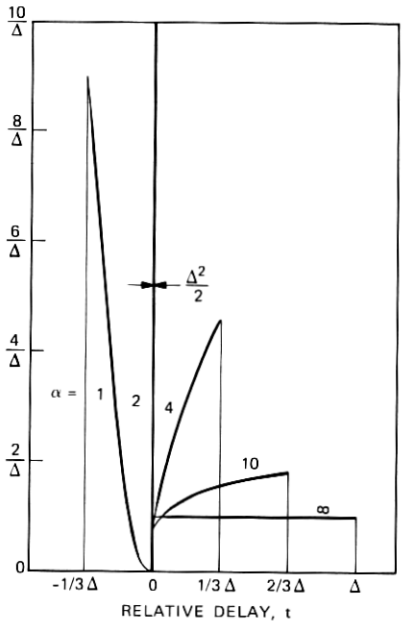

Fig. 6—Impulse response of multimode fibers having the profiles of Fig. 5.

extremely narrow for $\alpha \approx 2$, then broadens again, as α decreases further. For $\alpha < 2$, the high-order modes overtake the fundamental and arrive earlier.

In the vicinity of $\alpha = 2$, where both terms of (19) contribute, the impulse response is a rather complicated function. The most interesting of these cases is the one for which the impulse response has the narrowest possible width. This optimum condition arises for

$$\alpha_{\text{opt}} = 2 - 2\Delta , \tag{23}$$

which yields

$$t = \tfrac{1}{2}(\delta^2 - \Delta\delta). \tag{24}$$

In this case, the modes of highest and lowest order both arrive at the same time $t = 0$; all other modes are faster, the fastest one being determined by $\delta = \Delta/2$. It arrives at

$$t = -\frac{\Delta^2}{8}. \tag{25}$$

Equation (24) has two solutions for δ. Hence, (17) yields two values for the same t, indicating that two mode groups, a high and a lower order, contribute to the impulse response at every particular instant in time. By introducing δ into (17), differentiating with respect to t, and then adding the two contributions, we find the impulse response

$$\frac{4}{\Delta^2}\left(1 + \frac{8t}{\Delta^2}\right)^{-\frac{1}{2}}. \tag{26}$$

This function is plotted in Fig. 7. It peaks at $t = -\Delta^2/8$ and decreases towards $t = 0$. Because of the normalization introduced in (19), the absolute temporal width is

$$\frac{Ln_o}{c}\frac{\Delta^2}{8}. \tag{27}$$

The time slot in which a pulse of this kind can be transmitted is narrower than that, because 70 percent of the power is concentrated in the first half of the interval (27).

A practical implementation must, of course, allow for a certain tolerance or error in the profile, as a result of which the total width of the impulse response is likely to exceed (27). To obtain some indication of the pulse broadening as a result of this index deviation, we assume that the erroneous profile is still of the type (9), but has

$$\alpha = \alpha_{\text{opt}} + d\alpha. \tag{28}$$

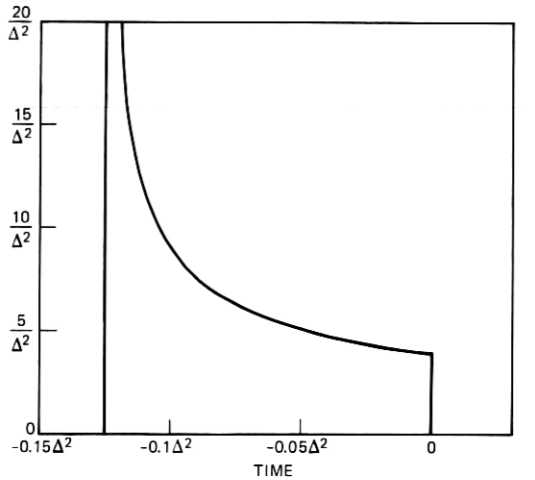

Fig. 7—Impulse response in the case of optimal profile shape.

The maximum index deviation from the optimum profile then appears approximately at

$$r = ae^{-\frac{1}{2}} \tag{29}$$

and has the value

$$dn_{\max} = d\alpha \frac{n_o \Delta}{2e}, \tag{30}$$

where e is the base of the natural logarithm. As a result of this profile error, the normalized width of the impulse response becomes

$$\tfrac{1}{8}(\Delta + \tfrac{1}{2}|d\alpha|)^2 \tag{31}$$

or, in absolute terms,

$$\frac{Ln_o}{8c}\left(\Delta + \frac{e}{n_o\Delta}|dn_{\max}|\right)^2. \tag{32}$$

Consider a guide with a maximum index $n_o = 1.5$ and an index variation $\Delta = 2$ percent. If the profile is optimal, mode delay should produce an effective broadening of only 0.25 ns/km. An index deviation of 10^{-4} from the optimal profile increases the broadening to 0.53 ns/km.

IV. NEAR- AND FAR-FIELD POWER DISTRIBUTION

We take again into account the fact that the core cross section measures many wavelengths in diameter. If this cross section is illuminated by an incoherent source (exciting all modes uniformly), the power

incident per unit solid angle at any point in the cross section is constant. To compute the power accepted by the fiber, we merely have to know the solid angle of acceptance at any point. We find this angle from the wave vector diagram of Fig. 2, which yields

$$\cos \theta(r) = \beta/k(r). \tag{33}$$

The maximum angle θ_c results for $\beta = \beta_c$; hence,

$$\cos \theta_c(r) = \frac{\beta_c}{k(r)} = \frac{n_c}{n(r)}. \tag{34}$$

Using this relation, we can define a local numerical aperture at the fiber front face

$$A(r) = n(r) \sin \theta_c(r) = [n^2(r) - n_c^2]^{\frac{1}{2}}. \tag{35}$$

The power accepted at r is then

$$p(r) = p(0) \frac{A^2(r)}{A^2(0)} = p(0) \frac{n^2(r) - n_c^2}{n^2(0) - n_c^2}. \tag{36}$$

If all modes propagate equally attenuated and without coupling, the

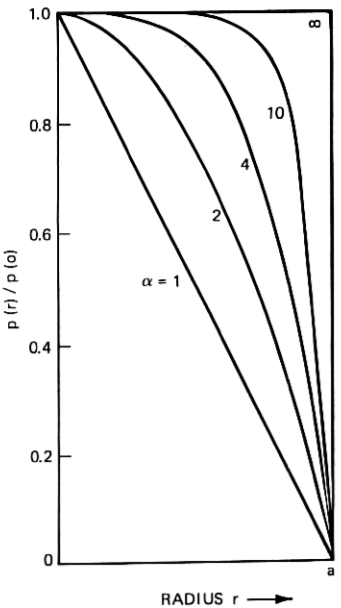

Fig. 8—Power distribution in the core of multimode fibers having the profiles of Fig. 5.

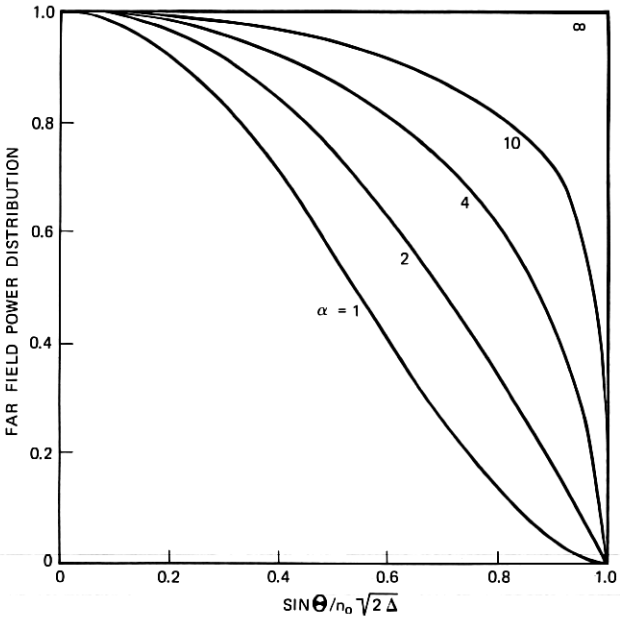

Fig. 9—Power distribution in the far field of multimode fibers having the profiles of Fig. 5.

same power distribution should hold for the fiber end face. The class of profiles described by (9) has

$$A(r) = n_o(2\Delta)^{\frac{1}{2}}[1 - (r/a)^\alpha]^{\frac{1}{2}} \tag{37}$$

and

$$p(r) = p(0)[1 - (r/a)^\alpha]. \tag{38}$$

The agreement between the profile plots (Fig. 5) and the near-field power plots (Fig. 8) is not a coincidence, but holds in general as long as the total index variation is small.

Under the conditions assumed here, every incremental area of the core cross section at the fiber end uniformly illuminates its cone of acceptance. For this reason, all those areas that have a numerical aperture

$$A(r) \geqq \sin\theta \tag{39}$$

contribute equally to the far-field power at θ. For the class of profiles described by (9), the areas contributing to θ are within a circle whose radius is obtained by solving (37) for r. Consequently,

$$P(\theta) = P(0)\left(1 - \frac{\sin^2\theta}{2n_o^2\Delta}\right)^{2/\alpha} \tag{40}$$

is the far-field power distribution. Figure 9 shows a plot of (40) for the profiles of Fig. 5. The uniform illumination for $\alpha = \infty$ changes to a parabolic distribution for $\alpha = 2$. All plots must be understood as the average power expected under the idealized conditions mentioned earlier. Monochromatic mode excitation results in mode interference phenomena and a local fine structure, which can greatly modify the average distribution considered here.

V. CONCLUSIONS

By assuming somewhat idealized conditions for mode excitation, coupling, and loss in a multimode fiber, we can isolate the influence of the index profile upon mode volume, near- and far-field power distribution, group delay, and impulse response. Surprisingly simple relations exist for a special class of profiles which comprises most multimode fibers of interest. Particular attention is given to a near-parabolic profile which accomplishes optimal delay equalization of all modes. If the (relative) index difference between center and periphery of this profile is Δ, mode delay broadens the impulse response by a fraction $\Delta^2/8$ of the total propagation time. This amounts to about 0.25 ns/km for $\Delta = 2$ percent. On the other hand, an index deviation of 10^{-4} from the optimal profile increases the broadening to 0.53 ns/km.

APPENDIX

Some Further Relations for the Group Velocity

The numerical evaluation of β as a function of μ, ν, and k_o and its subsequent differentiation to obtain τ are usually tedious and time-consuming. A substantial simplification results from a direct computation of τ by applying the operation

$$\tau = \frac{Ln_o}{c} \frac{\partial \mu / \partial k_o}{\partial \mu / \partial \beta} \tag{41}$$

to (3). The result is

$$\tau = \frac{L}{c} \frac{\int_{R_1}^{R_2} k(r) n(r) dr/u(r)}{\int_{R_1}^{R_2} \beta dr/u(r)}. \tag{42}$$

To understand the physical significance of this relation, consider a ray propagating along the fiber core of Fig. 2 in such a way that it has the direction of $k(r)$ at r. A line element along this ray is

$$ds = (dr^2 + r^2 d\phi^2 + dz^2)^{\frac{1}{2}} \tag{43}$$

and therefore

$$\frac{ds}{dr} = \frac{k(r)}{u(r)} \qquad \text{and} \qquad \frac{dz}{dr} = \frac{\beta}{u(r)}. \tag{44}$$

The condition $u(r) = dr = 0$ at R_1 and R_2 indicates a reflection (turnaround) of the ray. The ray performs periodic undulations between R_1 and R_2, simultaneously moving sideways in a helical fashion. By introducing (44) into (42), we obtain

$$\tau = L \frac{\oint n(r)ds/c}{\oint dz}, \tag{45}$$

where $\oint$ denotes integration over a full period of the ray. The denominator describes the axial length of one ray period, and the numerator the propagation time along the ray within this length. Multiplied by the fiber length, this ratio yields the total group delay. This result emphasizes the equivalence between ray theory and the zeroth-order WKB approach followed in this paper.

Within this order of approximation, the only quantities that depend on the wavelength are the mode numbers. Normalization of these numbers and subsequent transition to continuous variables eliminates the wavelength entirely; group velocity and impulse response are then independent of wavelength. More specifically, if we write

$$\rho = \mu/ak_o \qquad \text{and} \qquad \sigma = \nu/ak_o \tag{46}$$

and

$$n = n_o[1 - 2d(r)]^{\frac{1}{2}}, \tag{47}$$

eq. (3) assumes the form

$$\rho = \frac{1}{\pi a} \int_{R_1}^{R_2} [2\delta - 2d - (\sigma a/r)^2]^{-\frac{1}{2}} dr, \tag{48}$$

and (42) becomes

$$\tau = \frac{Ln_o}{c} (1 - 2\delta)^{-\frac{1}{2}} \frac{\int_{R_1}^{R_2} (1 - 2d)dr/[2\delta - 2d - (\sigma a/r)^2]^{\frac{1}{2}}}{\int_{R_1}^{R_2} dr/[2\delta - 2d - (\sigma a/r)^2]^{\frac{1}{2}}}. \tag{49}$$

These two equations are sufficient to calculate group velocity and impulse response in the case of large mode numbers.

REFERENCES

1. Miller, S. E., "Light Propagation in Generalized Lens-Like Media," B.S.T.J., *44*, No. 9 (November 1965), pp. 2017–2064.
2. Kawakami, S., and Nishizawa, T., "An Optical Waveguide with the Optimum Distribution of the Refractive Index with Reference to Waveform Distortion," IEEE Trans. Microwave Theory and Tech., *MTT-16* (October 1968), pp. 814–818.
3. Uchida, M., Furukawa, M., Kitano, I., Koisumi, K., and Matsumura, H., "A Light-Focusing Fibre Guide," IEEE J. Quan. Elec. (Digest of Technical Papers), *QE-5* (June 1969), p. 331.
4. Gloge, D., Chinnock, E. L., and Koizumi, K., "Study of Pulse Distortion in Selfoc Fibers," Elec. Letters, *8*, 21 (October 19, 1972), pp. 526–627.
5. Gloge, D., "Weakly Guiding Fibers," Appl. Opt., *10*, 10, pp. 2252–2258.
6. Gloge, D., and Marcatili, E. A. J., "Impulse Response of Fibers with Ring-Shaped Parabolic Index Distribution," B.S.T.J., *52*, No. 7 (September 1973), pp. 1161–1168.
7. Matsuhara, M., "Analysis of Electromagnetic-Wave Modes in Lens-Like Media," J. Opt. Soc. Am., *63*, 2 (February 1973), pp. 135–138.
8. Morse, P. M., and Feshbach, H., *Methods of Theoretical Physics*, New York: McGraw-Hill, 1953, p. 1092.